Simple models for the quick estimation of ground state splittings from hydrogen tunneling in alcohols and other compounds

-

Electronic Supplementary Information

Robert Medel*

Contents

*Institute of Physical Chemistry, University of Goettingen, Tammannstr. 6, 37077 Goettingen. Germany. E-mail: rmedel@gwdg.de

1 Scaled Eckart Barrier Model

By close inspection of the performance of the Eckart Barrier Model in Fig. 4 of the main document one notices that isotopologs typically have similar over- or underestimations. This supports the plausible expectation that isotopologs have more similar barrier shapes than chemically distinct species and thus also more akin deviations from the Eckart idealization. More similar errors in their quantum chemical evaluation likely also contribute. One can exploit this observation with eqn (S1). Herein Δ(Eckart) corresponds to the calculation through the Eckart Barrier Model, given by eqn (S2).

$$\Delta_{\mathrm{D}}(\mathrm{calc}) = \Delta_{\mathrm{H}}(\mathrm{exp})\frac{\Delta_{\mathrm{D}}(\mathrm{Eckart})}{\Delta_{\mathrm{H}}(\mathrm{Eckart})} \tag{S1}$$

$$\Delta(\mathrm{Eckart}) = \frac{\omega_0 hc}{\sqrt{\pi \mathrm{e}}} \exp\left[-\frac{2\pi}{|\omega_{\mathrm{i}}|}\left(V_0 - \sqrt{E_0 V_0}\right)\right] \tag{S2}$$

For deuterated alcohols the correlation between the experimental tunneling splittings and those estimated from their lighter isotopologs is shown in Fig. S1.

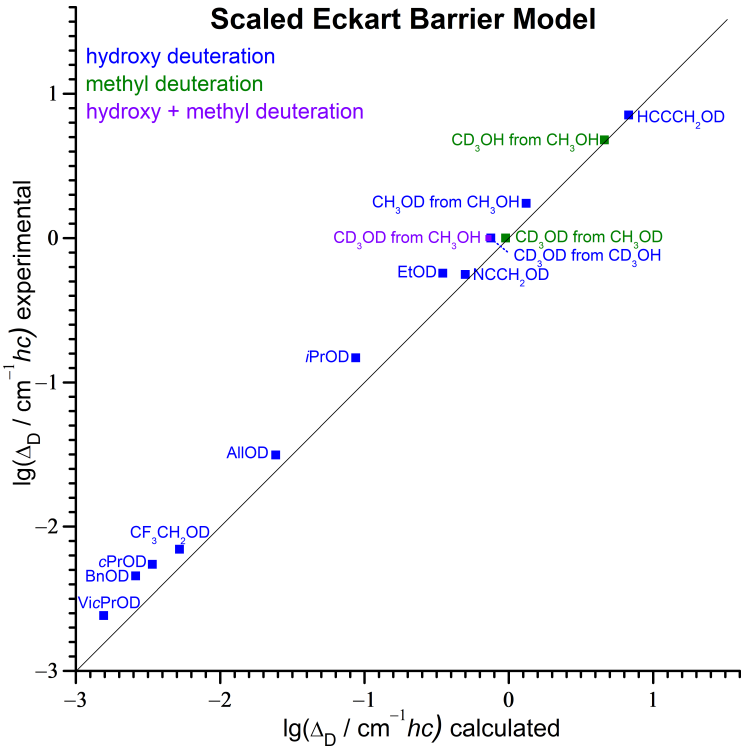

Figure S1: Correlation between the experimental tunneling splittings for deuterated alcohols and those calculated from their lighter isotopologs by the Scaled Eckart Barrier Model through eqn (S1). The diagonal line represents perfect agreement.

In all cases the splitting is slightly to moderately underestimated, showing that the Eckart Barrier Model overestimates the isotope effect. For methanol the effect from the smaller increase of the tunneling mass by deuteration of the methyl group is better anticipated than from deuteration of the hydroxy group. Interestingly, the effect of deuteration on benzyl alcohol is also reasonably well captured, making it the only simple model discussed in this work to do so. However, the very extensive error cancellation for this case might be at least partly accidental.

Taking only hydroxy deuteration into account and excluding BnOH, one obtains for the 10 data points MSDF = 1.39 and MAX = 1.7 for *i*PrOD. This can be compared to MSDF = 1.87

and MAX = 3.2 for *i*PrOD for the same alcohols in the original Eckart Barrier Model, showing the improvement.

With all values deviating in the same direction, it is tempting to employ a further empirical correction. A linear regression for the hydroxy deuteration data in Fig. S1 with a fixed slope of unity yields an intercept of 0.14, which converts to a scaling by factor 1.38. This is equivalent to moving all data points by 0.14 to the right in Fig. 1 for overall better agreement with the diagonal line. Using eqns (S3) and (S4) brings the deviations further down to MSDF = 1.14 and MAX = 1.32 for $HCCCH_2OD$.

$$\Delta_{\mathrm{D}}(\mathrm{calc}) = 1.38\Delta_{\mathrm{H}}(\exp)\frac{\Delta_{\mathrm{D}}(\mathrm{Eckart})}{\Delta_{\mathrm{H}}(\mathrm{Eckart})} \tag{S3}$$

$$\Delta_{\mathrm{H}}(\mathrm{calc}) = 1.38^{-1}\Delta_{\mathrm{D}}(\exp)\frac{\Delta_{\mathrm{H}}(\mathrm{Eckart})}{\Delta_{\mathrm{D}}(\mathrm{Eckart})} \tag{S4}$$

2 Performance overview

Table S1: Performance of the investigated models for the reproduction of tunneling splittings of alcohols. MSDF is the mean symmetric deviation factor, defined as the arithmetic average of the ratios between experiment and calculation taken as ≥ 1, and MAX is the maximum symmetric deviation factor. $n = 27$ is the full set of splittings given in Table 1 of the main document, with the exclusion of only BnOH/D. $n = 21$ is a subset of alcohols with more similar properties with the further exclusion of CH_3OH/D, $MeOCH_2OH$, CF_3CH_2OH/D and FCH_2OH. $n = 10$ are deuterated alcohols (expect BnOD) for which also the splitting of the protiated isotopolog is known, so that models for the isotope effect can be applied. $n = 77$ are isotopologic pairs of chemically very diverse systems with hydrogens tunneling, with the 10 pairs of alcohols forming a subset.

n	Model	eqn	MSDF	MAX
27	Eckart Barrier	(6)	1.75	4.9
27	Barrier Height	(9),(10)	1.50	3.0
27	Effective Barrier Height	(19),(20)	1.39	2.4
21	Eckart Barrier	(6)	1.65	2.6
21	Barrier Height	(9),(10)	1.39	2.3
21	Restricted Barrier Height	(15),(16)	1.21	1.5
21	Effective Barrier Height	(19),(20)	1.37	2.4
10	Eckart Barrier	(6)	1.87	3.2
10	Barrier Height	(10)	1.45	2.2
10	Effective Barrier Height	(20)	1.50	2.4
10	Scaled Eckart Barrier	(S4)	1.14	1.3
10	Mass Scaling	(25)	1.19	1.4
10	Direct Correlation	(27)	1.15	1.3
10	Universal Direct Correlation	(32)	1.25	1.6
77	Universal Direct Correlation	(32)	1.33	2.6

3 List of tunneling splittings in the Universal Direct Correlation Model

Table S2: Isotopologic pairs of experimental hydrogen tunneling splittings for diverse compounds reported in the literature and used in the Universal Direct Correlation Model. Given values are in $\mathrm{cm}^{-1}hc$ and were rounded to two leading digits. The list continues in Table 1 of the main document (excluding benzyl alcohol) and in Table S3.

category	system	Δ_{H}(exp)	Δ_{D}(exp)
thiol torsion	ethanethiol	$5.9{\cdot}10^{-2}$ [1]	$2.3{\cdot}10^{-3}$ [1]
	1-propanethiol	$5.4{\cdot}10^{-2}$ [2]	$1.9{\cdot}10^{-3}$ [2]
	1-butanethiol	$5.7{\cdot}10^{-2}$ [3]	$1.9{\cdot}10^{-3}$ [3]
	2-propyne-1-thiol	$2.3{\cdot}10^{-1}$ [4]	$1.3{\cdot}10^{-2}$ [4]
	2-propanethiol	$1.9{\cdot}10^{-2}$ [5]	$3.4{\cdot}10^{-4}$ [5]
	trifluoromethanethiol	$1.0{\cdot}10^{-1}$ [6]	$3.0{\cdot}10^{-3}$ [6]
	methylsilanethiol	$9.4{\cdot}10^{-2}$ [7]	$3.9{\cdot}10^{-3}$ [7]
selenol torsion	ethaneselenol	$3.6{\cdot}10^{-2}$ [8]	$1.3{\cdot}10^{-3}$ [8]
	2-propaneselenol	$1.2{\cdot}10^{-2}$ [9]	$1.7{\cdot}10^{-4}$ [9]
diol torsion	1,2-ethanediol $g'Ga$	$2.3{\cdot}10^{-1}$ [10]	$9.8{\cdot}10^{-3}$ [10]
	1,4-butanediol I	$2.1{\cdot}10^{-4}$ [11]	$4.6{\cdot}10^{-7}$ [11]
phenol torsion	phenol	$1.9{\cdot}10^{-3}$ [12]	$7.6{\cdot}10^{-6}$ [12]
	4-chlorophenol	$2.7{\cdot}10^{-3}$ [13]	$1.3{\cdot}10^{-5}$ [13]
	4-fluorophenol	$5.9{\cdot}10^{-3}$ [12]	$3.9{\cdot}10^{-5}$ [12]
thiophenol torsion	thiophenol	$2.7{\cdot}10^{-2}$ [14]	$3.7{\cdot}10^{-4}$ [14]
other torsion	hydrogen peroxide	$1.1{\cdot}10^{+1}$ [15]	1.9 [16]
other torsion	ethylene cation	$8.4{\cdot}10^{+2}$ [17]	$3.7{\cdot}10^{+2}$ [17]
other torsion	ethylamine	$3.9{\cdot}10^{-2}$ [18]	$9.8{\cdot}10^{-4}$ [18]
nitrogen inversion	ammonia	$7.9{\cdot}10^{-1}$ [19]	$5.3{\cdot}10^{-2}$ [20]
	methylamine	$9.7{\cdot}10^{-1}$ [21]	$7.6{\cdot}10^{-2}$ [21]
	ethylamine	$4.6{\cdot}10^{-2}$ [18]	$1.2{\cdot}10^{-3}$ [18]
	aniline	$4.1{\cdot}10^{+1}$ [22]	$1.3{\cdot}10^{+1}$ [22]
	ethylmethylamine	$6.6{\cdot}10^{-2}$ [23]	$2.2{\cdot}10^{-3}$ [23]
	dimethylamine	$8.8{\cdot}10^{-2}$ [24]	$3.6{\cdot}10^{-3}$ [24]
	cyanamide	$5.0{\cdot}10^{+1}$ [25]	$1.6{\cdot}10^{+1}$ [25]
	amino cyclobutane	$4.0{\cdot}10^{-1}$ [26]	$1.9{\cdot}10^{-2}$ [26]
	isocyanamide	$3.7{\cdot}10^{-1}$ [27]	$1.5{\cdot}10^{-2}$ [27]
	ammonia-argon	$7.6{\cdot}10^{-1}$ [28]	$4.8{\cdot}10^{-2}$ [28]
	2-aminopyridine	$8.7{\cdot}10^{+1}$ [29]	$3.9{\cdot}10^{+1}$ [29]
	hydrazine	$2.7{\cdot}10^{-1}$ [30]	$1.5{\cdot}10^{-2}$ [31]
oxygen inversion	hydronium	$5.5{\cdot}10^{+1}$ [32]	$1.5{\cdot}10^{+1}$ [33]
geared rotation	hydrogen fluoride dimer	$6.6{\cdot}10^{-1}$ [34]	$5.3{\cdot}10^{-2}$ [34]
	hydrogen chloride dimer	$1.5{\cdot}10^{+1}$ [35]	6.0 [36]
pseudorotation	methane cation	4.1 [37]	$3.5{\cdot}10^{-1}$ [37]
carbonic acid dimer	formic acid + propiolic acid	$9.7{\cdot}10^{-3}$ [38]	$1.2{\cdot}10^{-4}$ [39]
	acrylic acid dimer	$2.9{\cdot}10^{-2}$ [40]	$1.0{\cdot}10^{-3}$ [40]
	benzoic acid + formic acid	$1.8{\cdot}10^{-2}$ [41]	$2.8{\cdot}10^{-4}$ [41]

Table S3: Continuation of Table S2.

category	system	Δ_{H}(exp)	Δ_{D}(exp)
out-of-plane bending	$H_2O\cdots HF$	$6.4{\cdot}10^{+1}$ [42]	$3.2{\cdot}10^{+1}$ [42]
acceptor switching	water dimer	9.4 [43]	1.8 [43]
interchange (lower)	water dimer	$7.5{\cdot}10^{-1}$ [43]	$3.9{\cdot}10^{-2}$ [43]
bifurcation (lower)	water dimer	$2{\cdot}10^{-2}$ [43]	$2.3{\cdot}10^{-4}$ [43]
flip	water trimer	$4.4{\cdot}10^{+2}$ [43]	$2.1{\cdot}10^{2}$ [43]
bifurcation	water trimer	$9.6{\cdot}10^{-3}$ [43]	$1.7{\cdot}10^{-4}$ [43]
bifurcation	water + carbonmonoxide	$5.6{\cdot}10^{-1}$ [44]	$3.4{\cdot}10^{-2}$ [44]
solid solution in metal	manganese	$5.2{\cdot}10^{+1}$ [45]	$1.3{\cdot}10^{1}$ [45]
	niobium doped with oxygen	1.9 [46]	$1.6{\cdot}10^{-1}$ [46]
	niobium doped with nitrogen	1.4 [46]	$1.1{\cdot}10^{-1}$ [46]
rocking	vinyl radical	$5.4{\cdot}10^{-1}$ [47]	$4.0{\cdot}10^{-2}$ [47]
hydrogen transfer	malonaldehyde	$2.2{\cdot}10^{+1}$ [48]	2.9 [48]
	tropolone	$9.7{\cdot}10^{-1}$ [49]	$5.1{\cdot}10^{-2}$ [49]
	6-hydroxy-2-formylfulvene	$1.2{\cdot}10^{+2}$ [50]	$3.6{\cdot}10^{+1}$ [50]
ammonium reorientation	$(NH_4)_2SnCl_6$	$2.4{\cdot}10^{-2}$ [51]	$2.4{\cdot}10^{-4}$ [52]
ammonium torsion	$(NH_4)_2IrCl_6$	$9.3{\cdot}10^{+1}$ [53]	$3.1{\cdot}10^{+1}$ [53]
	$(NH_4)_2RuCl_6$	$7.0{\cdot}10^{+1}$ [54]	$3.9{\cdot}10^{+1}$ [54]
	$(NH_4)_2SnCl_6$	$1.3{\cdot}10^{+2}$ [54]	$4.2{\cdot}10^{+1}$ [54]
methyl torsion	nitromethane crystal 1 bar	$2.8{\cdot}10^{-1}$ [55]	$1.4{\cdot}10^{-2}$ [55]
	nitromethane crystal 4.8 kbar	$4.4{\cdot}10^{-1}$ [55]	$2.3{\cdot}10^{-2}$ [55]
	acetamide crystal	$2.6{\cdot}10^{-1}$ [56]	$9.5{\cdot}10^{-3}$ [56]
	$(CH_3)_2SnCl_2$ crystal	$2.6{\cdot}10^{-1}$ [57]	$2.1{\cdot}10^{-2}$ [57]
	$(CH_3COO)_2Cu{\cdot}H_2O$ crystal	$2.1{\cdot}10^{-3}$ [58]	$2.0{\cdot}10^{-5}$ [58]
	acetylsalicylic acid crystal	$9.8{\cdot}10^{-3}$ [59]	$9.0{\cdot}10^{-5}$ [59]
	toluene crystal	$2.0{\cdot}10^{-1}$ [60]	$8.9{\cdot}10^{-3}$ [60]

4 Further examples for the application of the Direct Correlation Model

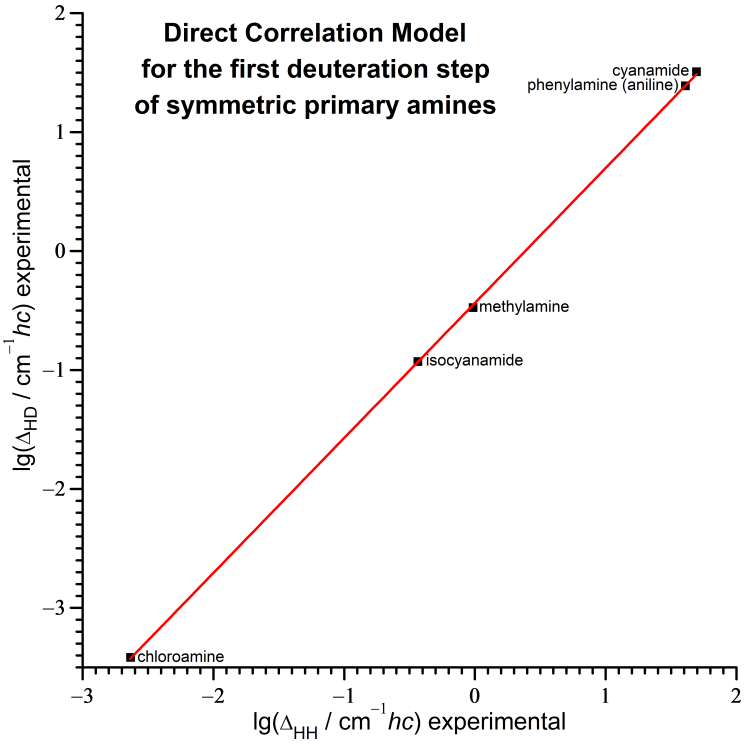

Figure S2: Correlation between the experimental inversion splittings of N-single-deuterated and N-protiated symmetric primary amines and amides. Used values with references are given in Table S4. $\lg\left(\Delta_{\mathrm{HD}}/\mathrm{cm}^{-1}hc\right) = 1.135 \cdot \lg\left(\Delta_{\mathrm{HH}}/\mathrm{cm}^{-1}hc\right) - 0.436$. MSDF = 1.026 and MAX = 1.058 for cyanamide.

Table S4: Experimental inversion splittings for N-protiated and N-single-deuterated symmetric primary amines, *i.e.* with both hydrogen atoms being equivalent in the inverting conformation. Values are rounded to two leading digits and given in $\mathrm{cm}^{-1}hc$.

system	Δ_{HH}(exp)	Δ_{HD}(exp)
cyanamide	$5.0{\cdot}10^{+1}$ [25]	$3.2{\cdot}10^{+1}$ [25]
aniline	$4.1{\cdot}10^{+1}$ [22]	$2.4{\cdot}10^{+1}$ [22]
methylamine	$9.7{\cdot}10^{-1}$ [21]	$3.3{\cdot}10^{-1}$ [61]
isocyanamide	$3.7{\cdot}10^{-1}$ [27]	$1.2{\cdot}10^{-1}$ [27]
chloroamine	$2.3{\cdot}10^{-3}$ [62]	$3.8{\cdot}10^{-4}$ [63]

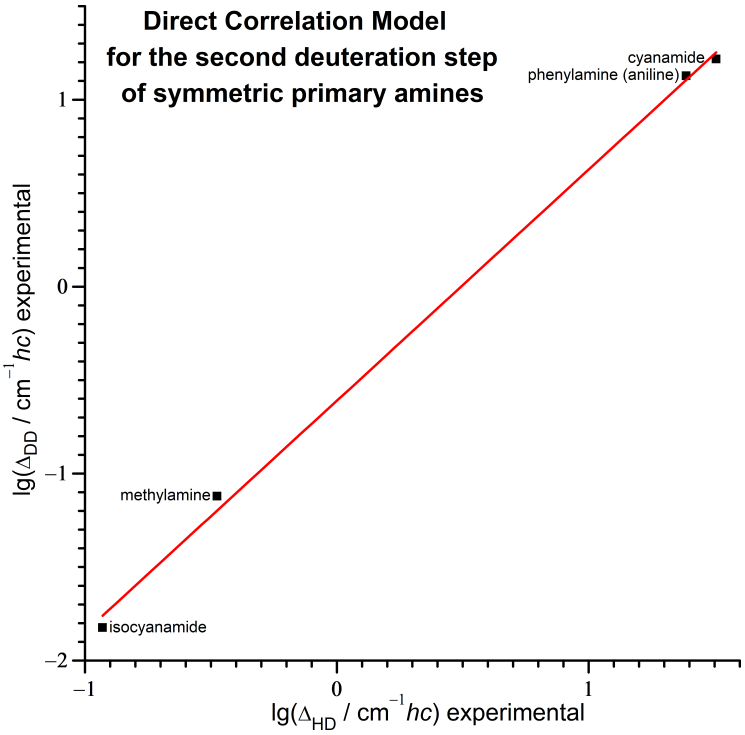

Figure S3: Correlation between the experimental inversion splittings of N-double-deuterated and N-single-deuterated symmetric primary amines and amides. Used values with references are given in Tables S2 and S4. $\lg\left(\Delta_{\mathrm{DD}}/\mathrm{cm}^{-1}hc\right) = 1.24 \cdot \lg\left(\Delta_{\mathrm{HD}}/\mathrm{cm}^{-1}hc\right) - 0.61$. MSDF = 1.12 and MAX = 1.19 for methylamine.

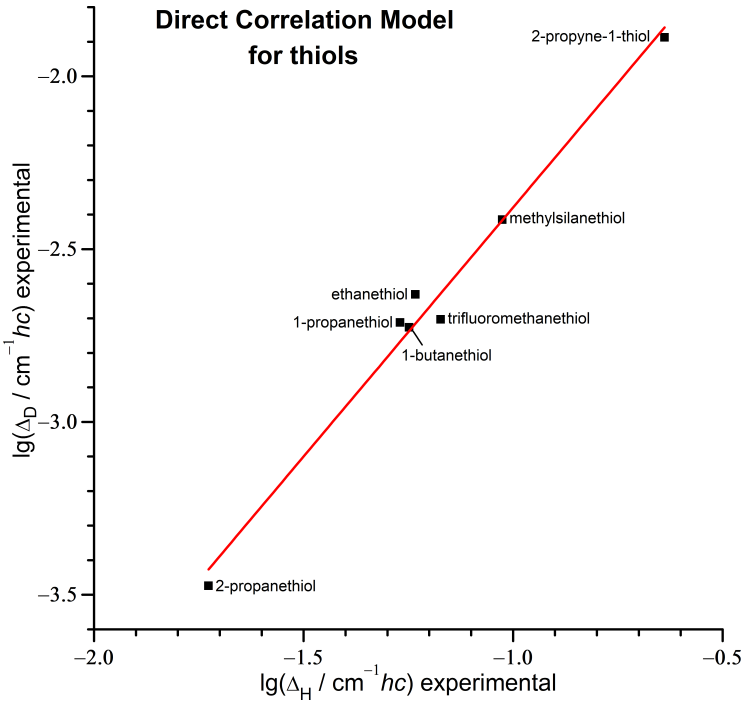

Figure S4: Correlation between the experimental tunneling splittings of deuterated and protiated thiols. Used values with references are given in Table S2. Values for trifluoromethanethiol were multiplied by 2/3. $\lg\left(\Delta_{\mathrm{D}}/\mathrm{cm}^{-1}hc\right) = 1.44 \cdot \lg\left(\Delta_{\mathrm{H}}/\mathrm{cm}^{-1}hc\right) - 0.94$. MSDF = 1.11 and MAX = 1.21 for ethanethiol.

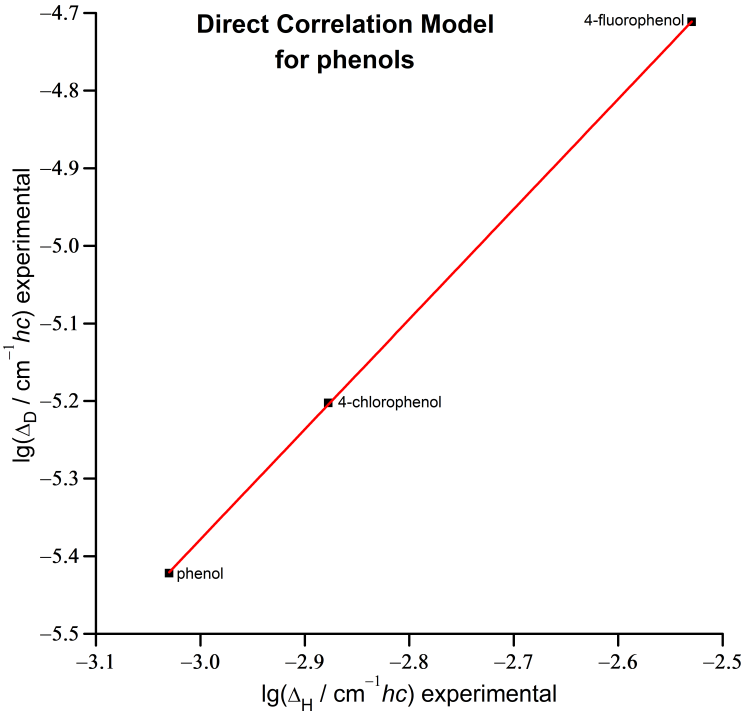

Figure S5: Correlation between the experimental tunneling splittings of deuterated and protiated phenols. Values with references given in Table S2 were multiplied with 1/2. $\lg\left(\Delta_{\mathrm{D}}/\mathrm{cm}^{-1}hc\right) = 1.419 \cdot \lg\left(\Delta_{\mathrm{H}}/\mathrm{cm}^{-1}hc\right) - 1.123$. MSDF = 1.0028 and MAX = 1.0042 for 4-chlorophenol.

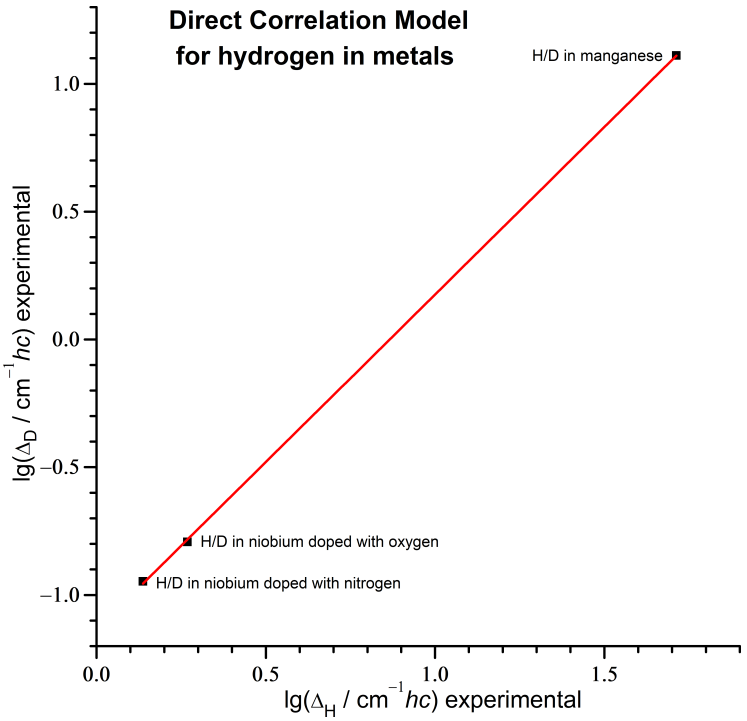

Figure S6: Correlation between the experimental tunneling splittings of solid solutions of hydrogen in metals. Values with references are given in Table S3. $\lg\left(\Delta_{\mathrm{D}}/\mathrm{cm}^{-1}hc\right) = 1.311 \cdot \lg\left(\Delta_{\mathrm{H}}/\mathrm{cm}^{-1}hc\right) - 1.135$. MSDF = 1.014 and MAX = 1.021 for H/D in niobium doped with oxygen.

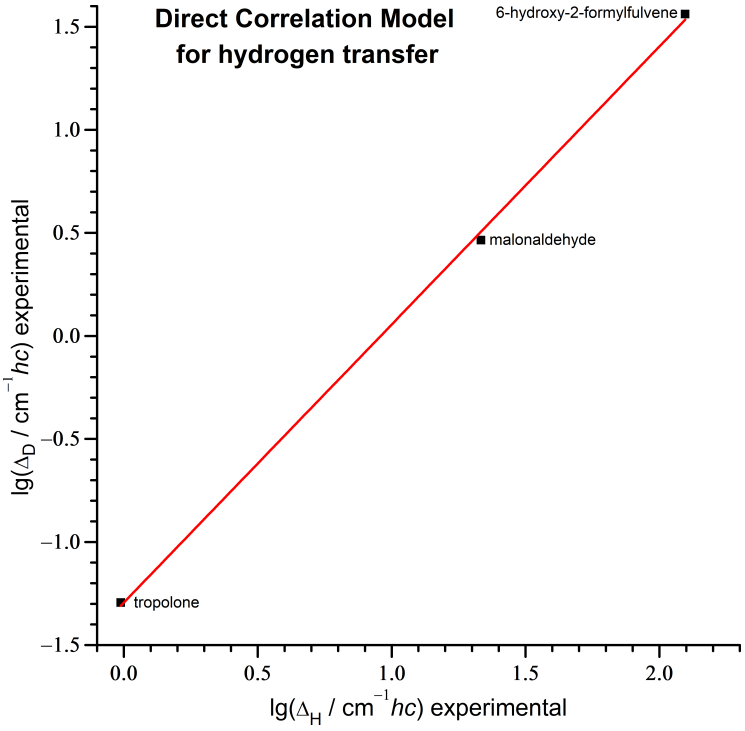

Figure S7: Correlation between the experimental tunneling splittings of hydrogen transfer system. Values with references are given in Table S3. $\lg\left(\Delta_{\mathrm{D}}/\mathrm{cm}^{-1}hc\right) = 1.35 \cdot \lg\left(\Delta_{\mathrm{H}}/\mathrm{cm}^{-1}hc\right) - 1.29$. MSDF = 1.07 and MAX = 1.10 for malonaldehyde.

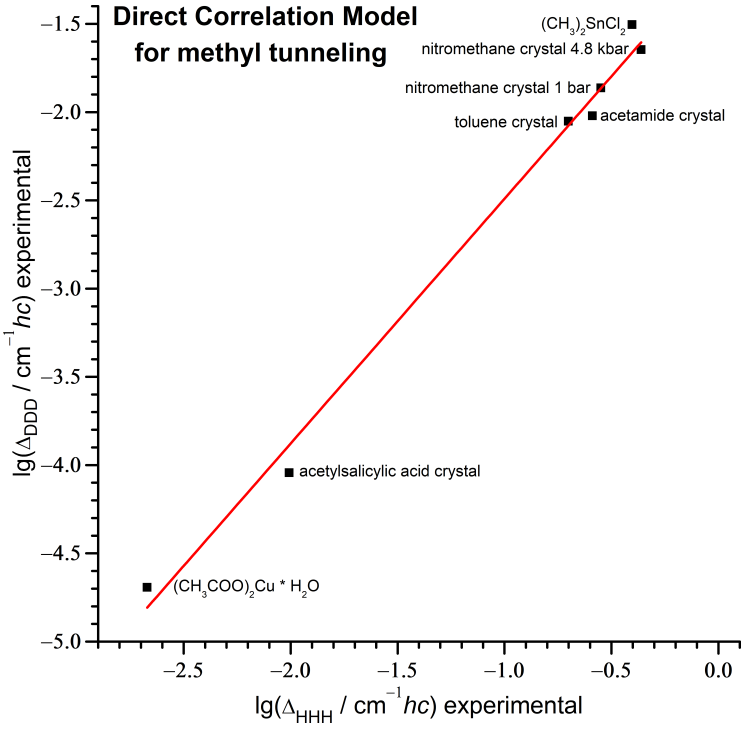

Figure S8: Correlation between the experimental tunneling splittings of system with methyl group tunneling. Values with references are given in Table S3. $\lg\left(\Delta_{\mathrm{D}}/\mathrm{cm}^{-1}hc\right) = 1.39 \cdot \lg\left(\Delta_{\mathrm{H}}/\mathrm{cm}^{-1}hc\right) - 1.10$. MSDF = 1.23 and MAX = 1.44 for $(CH_3)_2SnCl_2$.

5 Example inputs and outputs

Input and output files for the example methanol are provided as part of this supplementary information as separate files. Before calculating other alcohols it is recommended to do a quick rerun to check whether the expected result is reproduced as stated in the output file as well as in the included comment in the input file. Default settings might change in future versions of the software, so that adjustments to the input might become necessary. The inputs were tested with Gaussian 09 Rev. E.01 and Gaussian 16 Rev. A.03. The provided cartesian coordinates in the input files are the optimized values taken from the output files.

A spreadsheet for the application of the models is provided as a separate file as well, again with methanol as an example.

6 Discussion of metrics for the evaluation of model perfomance

Finding an appropriate metric to evaluate and compare performance between models is not trivial.

6.1 Mean absolute error (MAE)

With tunneling splittings spanning several orders of magnitude, common metrics for absolute errors, such as the *mean absolute error* (MAE, eqn (S5)), become meaningless.

$$\mathrm{MAE} = \frac{1}{n}\sum_{j}^{n} |\Delta_j(\mathrm{exp}) - \Delta_j(\mathrm{calc})| \tag{S5}$$

An overestimation by $0.1\,\mathrm{cm}^{-1}hc$ represents pinpoint accuracy for $HCCCCH_2OH$ ($\Delta = 21.8\,\mathrm{cm}^{-1}hc$), but very poor performance for CF_3CH_2OD ($\Delta = 0.007\,\mathrm{cm}^{-1}hc$), so these two results should not contribute equally to the sum of errors.

6.2 Mean absolute percentage error (MAPE)

A common metric for relative errors is the *mean absolute percentage error* (MAPE, eqn (S6)).

$$\mathrm{MAPE} = \frac{100\%}{n}\sum_{j}^{n} \frac{|\Delta_j(\mathrm{exp}) - \Delta_j(\mathrm{calc})|}{\Delta_j(\mathrm{exp})} \tag{S6}$$

It works well for small relative errors but for larger ones the metric shows pronounced asymmetry. An overestimation by a factor of two is twice as heavily penalized ($|+100\%|$) as an underestimation by the same factor ($|-50\%|$), while they arguably should be valued the same, at least when preferring a multiplicative scale.

6.3 Symmetric mean absolute percentage error (SMAPE)

One metric in use to solve the symmetry problem is the *symmetric mean absolute percentage error* (SMAPE, eqn (S7)), which uses instead the average of the calculated and experimental value as the reference in the denominator.[64,65]

$$\mathrm{SMAE} = \frac{100\%}{n}\sum_{j}^{n} \frac{|\Delta_j(\mathrm{exp}) - \Delta_j(\mathrm{calc})|}{[\Delta_j(\mathrm{exp}) + \Delta_j(\mathrm{calc})]/2} \tag{S7}$$

However, it is hard to interpret. The previous example of a model being constantly a factor two off target results in an odd value of SMAE = 67%. This metric is also very forgiving to larger errors. A strong over- or underestimation by a factor of 10 yields a penalty of 164%, which is only about four times as large as for an over- or underestimation by a far more acceptable factor of 1.5 (40%). As a matter of opinion, this might be seen as 'robustness' or 'ignorance' of the metric to outliers.

6.4 Mean absolute geometric error (MAGE)

Easier interpretable is the *mean absolute geometric error* (MAGE, eqn (S8)).[66]

$$\mathrm{MAGE} = \exp\left[\frac{1}{n}\sum_{j}^{n}\left|\ln\left(\frac{\Delta_j(\mathrm{exp})}{\Delta_j(\mathrm{calc})}\right)\right|\right] \tag{S8}$$

It can be rationalized as the geometric mean of ratios between calculated and experimental splittings, when always the smaller one is used in the denominator, so that ratios ≥ 1 result. MAGE is also the MAE of the logarithmized tunneling splittings back converted to obtain a 'typical' ratio between calculation and experiment.

It is as well rather forgiving to larger errors due to the logarithmic scaling. For the discussed example, the deviation by a factor of 10 is penalized $\ln(10)/\ln(1.5) \approx 5.7$ times as strongly as the one with a factor of 1.5.

6.5 Mean symmetric deviation factor (MSDF) and mean normalized absolute factor error (MNAFE)

Arguably even easier interpretable and more intuitive than MAGE is the *mean symmetric deviation factor* (MSDF, eqn (S9)).

$$\mathrm{MSDF} = \frac{1}{n}\sum_{j}^{n} \exp\left|\ln\left(\frac{\Delta_j(\mathrm{exp})}{\Delta_j(\mathrm{calc})}\right)\right| \tag{S9}$$

This metric was used before in a mean and median version.[67] It is also closely related to the *mean normalized absolute factor error* MNAFE (eqn (S10)).[68]

$$\mathrm{MNAFE} = \frac{1}{n}\sum_{j}^{n} \left[\exp\left|\ln\left(\frac{\Delta_j(\mathrm{exp})}{\Delta_j(\mathrm{calc})}\right)\right| - 1\right] \tag{S10}$$

Back converting the logarithmic deviations before the averaging (and not after as with MAGE) has some advantages. MSDF can be rationalized as the arithmetic (instead of the geometric) mean of the ratios between calculated and experimental values. This is equivalent to arithmetically averaging relative or percentage errors of tunneling splittings (as it is done with MNAFE). E.g., ratios of 1.80 (80%) and 1.20 (20%) will arithmetically average to 1.50 (50%) instead geometrically to 1.47 (47%) with MAGE. MSDF and MNAFE are thus closely related to a symmetrized MAPE with a flexible denominator containing always the smaller value of either $\Delta_j(\mathrm{exp})$ or $\Delta_j(\mathrm{calc})$ as reference.

MSDF and MNAFE penalize larger relative errors more heavily and more intuitively than both SMAPE and MAGE. A deviation by a factor of 10 weights 18 times as much as a deviation by a factor of 1.5, as one would intuitively expect from the associated percentage errors of 900%/50% = 18.

So why prefer MSDF over MNAFE (optionally multiplied by 100%)? The relative errors contributing to MNAFE have the problem that they refer to either $\Delta_j(\mathrm{exp})$ or $\Delta_j(\mathrm{calc})$, depending on which value is smaller, to reach the desired symmetry. This needs elaboration and special attention of the reader, as values of MNAFE could be easily confused with those of the commonly used MAPE. A stated underestimation by 200% is hard to understand and could be easily misinterpreted as the calculated value having the wrong sign. In a multiplicative system the desired symmetry arises more natural, which is reflected in the language. It is common to state an underestimation by a factor of 3, even though a factor of 1/3 would be arguably more correct.

7 Computed quantities for additional alcohols

Table S5: Calculated barrier heights with (V_0) and without (V_{el}) harmonic vibrational zero-point correction, as well as calculated harmonic torsional wavenumbers for the *gauche* equilibrium geometry ω_0 and for the transition state ω_{i} of alcohols with a protiated (index H) or deuterated (index D) hydroxy group. Splittings and barrier heights are given in $\mathrm{cm}^{-1}hc$, wavenumbers in cm^{-1}. The B3LYP-D3(BJ)/may-cc-pVTZ level was used.

alcohol	$V_{0,\mathrm{H}}$	$V_{0,\mathrm{D}}$	V_{el}	$\omega_{0,\mathrm{H}}$	$\omega_{0,\mathrm{D}}$	$\omega_{\mathrm{i,H}}$	$\omega_{\mathrm{i,D}}$	$\frac{\omega_{\mathrm{i,H}}^2}{\omega_{\mathrm{i,D}}^2}$
$NCCMe_2OH$	471	467	452	313	244	299i	223i	1.80
1PrOH Tg	421	407	398	275	193	302i	228i	1.76
1BuOH TTg	411	396	387	277	195	300i	226i	1.76

References

[1] J. Nakagawa, K. Kuwada and M. Hayashi, *Bull. Chem. Soc. Jpn.*, 1976, **49**, 3420–3432.

[2] J. Nakagawa and M. Hayashi, *J. Mol. Spectrosc.*, 1981, **85**, 327–340.

[3] Y. Kawashima, Y. Tanaka, T. Uzuyama and E. Hirota, *J. Phys. Chem. A*, 2021, **125**, 1166–1183.

[4] A. Mirri, F. Scappini, R. Cervellati and P. Favero, *J. Mol. Spectrosc.*, 1976, **63**, 509–520.

[5] J. H. Griffiths and J. E. Boggs, *J. Mol. Spectrosc.*, 1975, **56**, 257–269.

[6] A. Cox, C. Rego and R. Stevens, *J. Mol. Struct.*, 1990, **223**, 185–205.

[7] J. Nakagawa and Y. Miyake, *J. Mol. Spectrosc.*, 1986, **119**, 201–213.

[8] J. Nakagawa, H. Okutani and M. Hayashi, *J. Mol. Spectrosc.*, 1982, **94**, 410–425.

[9] J. Nakagawa, A. Nagayama and M. Hayashi, *J. Mol. Spectrosc.*, 1983, **99**, 415–430.

[10] D. Christen, L. Coudert, R. Suenram and F. Lovas, *J. Mol. Spectrosc.*, 1995, **172**, 57–77.

[11] L. Evangelisti, Q. Gou, L. Spada, G. Feng and W. Caminati, *Chem. Phys. Lett.*, 2013, **556**, 55–58.

[12] N. Larsen and F. Nicolaisen, *J. Mol. Struct.*, 1974, **22**, 29–43.

[13] N. Larsen, *J. Mol. Struct.*, 1986, **144**, 83–99.

[14] N. W. Larsen and L. Schulz, *J. Mol. Struct.*, 2009, 10.

[15] P. Helminger, W. C. Bowman and F. C. De Lucia, *J. Mol. Spectrosc.*, 1981, **85**, 120–130.

[16] R. H. Hunt and R. A. Leacock, *J. Chem. Phys.*, 1966, **45**, 3141–3147.

[17] S. Willitsch, U. Hollenstein and F. Merkt, *J. Chem. Phys.*, 2004, **120**, 1761–1774.

[18] E. Fischer and I. Botskor, *J. Mol. Spectrosc.*, 1984, **104**, 226–247.

[19] Š. Urban, V. Špirko, D. Papoušek, J. Kauppinen, S. Belov, L. Gershtein and A. Krupnov, *J. Mol. Spectrosc.*, 1981, **88**, 274–292.

[20] L. Fusina, G. di Lonardo and J. Johns, *J. Mol. Spectrosc.*, 1985, **112**, 211–221.

[21] K. Takagi and T. Kojima, *J. Phys. Soc. Jpn.*, 1971, **30**, 1145–1157.

[22] R. Kydd and P. Krueger, *Chem. Phys. Lett.*, 1977, **49**, 539–543.

[23] R. Penn and J. E. Boggs, *J. Mol. Spectrosc.*, 1973, **47**, 340–346.

[24] J. E. Wollrab and V. W. Laurie, *J. Chem. Phys.*, 1968, **48**, 5058–5066.

[25] Z. Kisiel, A. Kraśnicki, W. Jabs, E. Herbst, B. P. Winnewisser and M. Winnewisser, *J. Phys. Chem. A*, 2013, **117**, 9889–9898.

[26] L. B. Favero, B. Velino, A. Maris and W. Caminati, *J. Mol. Struct.*, 2002, **612**, 357–367.

[27] M. Winnewisser and J. Reinstaedtler, *J. Mol. Spectrosc.*, 1986, **120**, 28–48.

[28] J. Loreau, J. Liévin, Y. Scribano and A. van der Avoird, *J. Chem. Phys.*, 2014, **141**, 224303.

[29] R. Kydd, *Spectrochim. Acta, Part A Mol. Spectrosc.*, 1979, **35**, 409–413.

[30] S. Tsunekawa and T. Kojima, *J. Phys. Soc. Jpn.*, 1980, **49**, 1957–1964.

[31] S. Tsunekawa and T. Kojima, *J. Phys. Soc. Jpn.*, 1978, **44**, 1925–1930.

[32] S. Yu, B. J. Drouin, J. C. Pearson and H. M. Pickett, *Astrophys. J. Suppl. Ser.*, 2009, **180**, 119–124.

[33] M. Araki, H. Ozeki and S. Sato, *Mol. Phys.*, 1999, **97**, 177–183.

[34] J. T. Farrell, M. A. Suhm and D. J. Nesbitt, *J. Chem. Phys.*, 1996, **104**, 9313–9331.

[35] M. D. Schuder, C. M. Lovejoy, R. Lascola and D. J. Nesbitt, *J. Chem. Phys.*, 1993, **99**, 4346–4362.

[36] M. D. Schuder, D. D. Nelson and D. J. Nesbitt, *J. Chem. Phys.*, 1993, **99**, 5045–5060.

[37] H. J. Wörner, X. Qian and F. Merkt, *J. Chem. Phys.*, 2007, **126**, 144305.

[38] S. G. Kukolich, E. G. Mitchell, S. J. Carey, M. Sun and B. A. Sargus, *J. Phys. Chem. A*, 2013, **117**, 9525–9530.

[39] M. Sun, Y. Wang, S. J. Carey, E. G. Mitchell, J. Bowman and S. G. Kukolich, *J. Chem. Phys.*, 2013, **139**, 084316.

[40] G. Feng, L. B. Favero, A. Maris, A. Vigorito, W. Caminati and R. Meyer, *J. Am. Chem. Soc.*, 2012, **134**, 19281–19286.

[41] L. Evangelisti, P. Écija, E. J. Cocinero, F. Castaño, A. Lesarri, W. Caminati and R. Meyer, *J. Phys. Chem. Lett.*, 2012, **3**, 3770–3775.

[42] Z. Kisiel, A. C. Legon and D. J. Millen, *Proc. R. Soc. Lond. A*, 1982, **381**, 419–442.

[43] J. O. Richardson, S. C. Althorpe and D. J. Wales, *J. Chem. Phys.*, 2011, **135**, 124109.

[44] R. Bumgarner, S. Suzuki, P. A. Stockman, P. G. Green and G. A. Blake, *Chem. Phys. Lett.*, 1991, **176**, 123–127.

[45] V. E. Antonov, B. Dorner, V. K. Fedotov, G. Grosse, A. S. Ivanov, A. I. Kolesnikov, V. V. Sikolenko and F. E. Wagner, *J. Alloys Compd.*, 2002, 5.

[46] P. Gutsmiedl, M. Schiekhofer, K. Neumaier and H. Wipf, in: Quantum Aspects of Molecular Motions in Solids, Berlin, Heidelberg, 1987, pp. 158–162.

[47] K. Tanaka, M. Hayashi, M. Ohtsuki, K. Harada and T. Tanaka, *J. Chem. Phys.*, 2009, **131**, 111101.

[48] S. L. Baughcum, Z. Smith, E. B. Wilson and R. W. Duerst, *J. Am. Chem. Soc.*, 1984, **106**, 2260–2265.

[49] J. C. Keske, W. Lin, W. C. Pringle, S. E. Novick, T. A. Blake and D. F. Plusquellic, *J. Chem. Phys.*, 2006, **124**, 074309.

[50] Z. N. Vealey, L. Foguel and P. H. Vaccaro, *J. Phys. Chem. Lett.*, 2018, **9**, 4949–4954.

[51] M. Prager, W. Press, B. Alefeld and A. Hüller, *J. Chem. Phys.*, 1977, **67**, 5126–5132.

[52] L. P. Ingman, E. Koivula, Z. T. Lalowicz, M. Punkkinen and E. E. Ylinen, *Z. Für Phys. B Condens. Matter*, 1990, **81**, 175–181.

[53] Y. Kume and T. Asaji, *Z. Für Naturforschung A*, 2002, **57**, 504–508.

[54] Y. Kume, D. Amino and T. Asaji, *J. Mol. Struct.*, 2013, **1043**, 1–6.

[55] S. F. Trevino, *in: Quantum Aspects of Molecular Motions in Solids*, Springer Berlin Heidelberg, Berlin, Heidelberg, 1987, vol. 17, pp. 9–18.

[56] A. Heidemann, M. Prager and M. Monkenbusch, *Z. Physik B - Condensed Matter*, 1989, **76**, 77–88.

[57] J. Stanislawski, M. Prager and W. Häusler, *Phys. B Condens. Matter*, 1989, **156-157**, 356–358.

[58] Z. T. Lalowicz, U. Werner and W. Müller-Warmuth, *Z. Für Naturforschung A*, 1988, **43**, 219–227.

[59] M. Johnson, B. Frick and H. Trommsdorff, *Chem. Phys. Lett.*, 1996, **258**, 187–193.

[60] D. Cavagnat, A. Magerl, C. Vettier and S. Clough, *J. Phys. C: Solid State Phys.*, 1986, **19**, 6665–6672.

[61] N. Ohashi, M. Oda and K. Takagi, *J. Mol. Spectrosc.*, 1991, **145**, 180–191.

[62] G. Cazzoli and D. Lister, *J. Mol. Spectrosc.*, 1973, **45**, 467–474.

[63] E. Masuko, Y. Hamada, A. Mizoguchi, H. Fukushi, N. Kuze and T. Sakaizumi, *J. Mol. Spectrosc.*, 2009, **253**, 77–87.

[64] J. S. Armstrong, *Long-range forecasting: from crystal ball to computer*, Wiley, New York, 2nd edn, 1985.

[65] S. Makridakis, *Int. J. Forecast.*, 1993, **9**, 527–529.

[66] S. Jachner, G. Boogaart and T. Petzoldt, *J. Stat. Soft.*, 2007, **22**, 1–30.

[67] M. Hunger and P. Döll, *Hydrol. Earth Syst. Sci.*, 2008, **12**, 841–861.

[68] S. Yu, B. Eder, R. Dennis, S.-H. Chu and S. E. Schwartz, *Atmos. Sci. Lett.*, 2006, **7**, 26–34.